Laboratory Investigation (2020) 100:438–453
https://doi.org/10.1038/s41374-019-0331-9

ARTICLE

ETS2 promotes epithelial-to-mesenchymal transition in renal fibrosis by targeting JUNB transcription

Fang Yao[1,2] · Xiaojing Wang[2] · Zhong-Kai Cui[1] · Haibing Lan[3] · Xiaolan Ai[2] · Qiancheng Song[1] · Zhenguo Chen[1] · Jun Yang[1] · Bingyi Wu[2] · Xiaochun Bai[1]

Received: 26 January 2019 / Revised: 16 August 2019 / Accepted: 23 September 2019 / Published online: 22 October 2019

Abstract

Epithelial-to-mesenchymal transition (EMT) plays an important role in the progression of renal tubulointerstitial fibrosis, a common mechanism leading to end-stage renal failure. V-ets erythroblastosis virus E26 oncogene homolog 2 (ETS2), a transcription factor, exhibits diverse roles in pathogenesis; however, its role in renal fibrosis is not yet fully understood. In this study, we detected the expression of ETS2 in an animal model of renal fibrosis and evaluated the potential role of ETS2 in tubular EMT induced by TGF-β1. We found that ETS2 and profibrogenic factors, alpha-smooth muscle actin (α-SMA) and fibronectin (FN), were significantly increased in the unilateral ureteral obstruction (UUO)-induced renal fibrosis model in mice. In vitro, TGF-β1 induced a high expression of ETS2 dependent on Smad3 and ERK signaling pathway in human proximal tubular epithelial cells (HK2). Knockdown of ETS2 abrogated TGF-β1-mediated expression of profibrogenic factors vimentin, α-SMA, collagen I, and FN in HK2 cells. Mechanistically, ETS2 promoted JUNB expression in HK2 cells after TGF-β1 stimulation. Furthermore, luciferase and Chromatin Immunoprecipitation (ChIP) assays revealed that the binding of ETS2 to three EBS motifs on the promoter of JUNB triggered its transcription. Notably, silencing JUNB reversed the ETS2-induced upregulation of the profibrogenic factors in HK2 cells after TGF-β1 stimulation. These findings suggest that ETS2 mediates TGF-β1-induced EMT in renal tubular cells through JUNB, a novel pathway for preventing renal fibrosis.

Introduction

Chronic kidney disease (CKD) is an increasingly serious health problem, affecting about 13% population worldwide [1]. Renal fibrosis is a prominent pathological feature of various etiologies of CKDs. The severity of renal fibrosis is highly associated with the degree of renal dysfunction and the risk for renal failure progression [2, 3]. The main characteristic features of renal fibrosis include excessive inflammatory cell infiltration, interstitial fibroblast proliferation, and deposition of extracellular matrix (ECM) [2, 4–6].

Epithelial-to-mesenchymal transition (EMT) of renal tubular epithelial cells plays a significantly important role in the progression of renal fibrosis [7, 8]. Transforming growth factor β1 (TGF-β1), a principal profibrogenic cytokine, mediates the transcription of downstream target genes through activation of Smad-dependent or -independent signaling pathways, resulting in the EMT of renal tubular epithelial cells to aggravate renal fibrosis [9–11]. Although mounting studies have made progress in unveiling the mechanism of EMT programming, the molecular mechanism of TGF-β1-mediated EMT during renal fibrosis is largely unclarified.

V-ets erythroblastosis virus E26 oncogene homolog 2 (ETS2), a member of conserved transcription factors of the ETS family, has an E26 transformation-specific sequence (Ets) domain that interacts with specific core GGAA/T

✉ Bingyi Wu
wubingyi66@126.com

✉ Xiaochun Bai
baixc15@smu.edu.cn

[1] Department of Cell Biology, School of Basic Medical Sciences, Southern Medical University, Guangzhou 510515, China

[2] Research Center of Clinical Medicine, Nanfang Hospital, Southern Medical University, Guangzhou 510515 Guangdong, China

[3] Department of the Intensive Care Unit, The Second Affiliated Hospital of Nanchang University, Nanchang 330006 Jiangxi, China

sequence located in the promoter regions of target genes, through which the transcription of numerous genes is regulated [12, 13]. ETS2 is known to be involved in a variety of cellular functions, including apoptosis, proliferation, transformation, migration, and angiogenesis, in response to different extracellular signal molecules [14, 15]. Numerous studies have reported that ETS2 is linked with the extracellular matrix remodeling through regulating the expression of matrix metalloproteinases (MMPs) and ECM proteins, affecting the development of tumor, wound repair, and cardiovascular diseases [16–18]. In addition, the activation of ETS2 via phosphorylation at threonine-72 exacerbates murine pulmonary fibrosis [19, 20]. A recent report shows ETS2 is upregulated in renal cell carcinoma to promote the migration and invasion of renal carcinoma cells [21]. Considering tumor metastasis, lung and renal fibrosis all have EMT pathologies; those clues lead us to hypothesize that ETS2 plays a role in EMT during renal fibrosis, which has not yet been investigated.

In this study, we revealed that ETS2 was significantly upregulated in mouse kidneys with unilateral ureteral obstruction (UUO)-induced renal fibrosis, as well as in TGF-β1-treated HK2 cells. Furthermore, ETS2 directly modulated the transcription of JUNB to upregulate profibrotic factors, contributing to TGF-β1-induced EMT in HK2 cells. This study suggests that ETS2 may be a potential target for treatment of renal fibrosis.

Materials and methods

Animal experiments

All animal experiments were performed according to the Animal Care and Committee of Southern Medical University, and conformed to the Guidelines for the Care and Use of Laboratory Animals of the National Institute of Health. Male C57B/L6 mice (weighing 20–22 g, 8-week-old) were anaesthetized with pentobarbital (70 mg/kg) via intraperitoneal injection, and then randomly assigned to the sham-operated and UUO-treated groups ($n = 6$ for each group). Ureteral obstruction was executed by the double ligation of the left ureter using 4-0 silk via a midline abdominal incision. Mice in the sham group were subjected to the same operations except ureteral ligation. Kidney tissues were harvested at day 7 after surgery.

Immunohistochemical staining for kidney tissues

Mouse kidneys were fixed in 10% buffered formalin, embedded in paraffin, and sectioned (3 μm). Sections were deparaffinated, rehydrated, and performed to antigen retrieval in 0.01 M sodium citrate buffer (pH 6.0). After blocking for 1 h at room temperature, the sections were incubated with primary antibodies overnight at 4 °C, followed by incubation with the horseradish peroxidase–conjugated secondary antibody (Zhongshanjinqiao, China) and then stained with 3,3-diaminobenzidine (DAB) (Zhongshanjinqiao). PBS instead of primary antibodies was used as a negative control. Images were obtained with an Olympus BX51 microscope (Tokyo, Japan).

Cell culture

The human renal tubular cell line HK2 and Human embryonic kidney cell line 293 T (HEK293T) were obtained from the Cell Bank of Type Culture Collection (Chinese Academy of Sciences, Shanghai, China). HK2 cells were cultured in DMEM/F12 supplemented with 10% fetal bovine serum (Invitrogen, Carlsbad, CA). HEK293T cells were cultured in high-glucose DMEM supplemented with 10% FBS. All cells were incubated in a humidified incubator of 5% CO_2 at 37 °C. HK2 cells were serum-starved for 12 h and subsequently treated with TGF-β1 (R&D Systems, Minneapolis, MN) or various inhibitors (Selleck Chemicals, Houston, TX) in serum-free DMEM/F12 medium as designed.

siRNA and plasmids transfection

The siRNAs targeting Smad3, ERK, JNK, P38, ETS2, and JUNB were purchased from Genepharma Biotechnology (Shanghai, China). Cells were cultured to 40% confluence, and transfected with scramble control siRNA or targeted siRNA using Lipofectamine® RNAiMAX Transfection Reagent (Invitrogen) for 24 or 48 h according to the manufacturer's instructions. The media were replaced with fresh serum-free DMEM/F12 containing TGF-β1 (5 ng/ml) for another 24 h. The sequences of siRNAs are listed in Table 1.

Western blot analysis

Kidney tissues and cells were extracted with RIPA buffer (KeyGEN biotech, Nanjing, China). Protein concentrations were determined using the BCA assay (Biocolors, Shanghai, China). Proteins (30 μg) separated by 10% SDS-PAGE were transferred to PVDF membranes (Bio-Rad, Hercules, CA). After blocking, membranes were incubated with primary antibodies overnight at 4 °C and subsequently incubated with IRDye800-conjugated secondary antibodies (Rockland Immunochemical, Gilbertsville, PA) for 1 h at room temperature. All protein bands and densitometry analyses were detected with an Odyssey Infrared Image System (LI-COR Biosciences, Licoln, NE). The primary

antibodies were used as follows: anti-ETS2 was gifted from Profession Peng Wang; anti-JUNB, anti-N-cadherin, anti-E-cadherin, anti-vimentin, anti-claudin1, anti-phospho-Smad3, anti-Smad3, anti-phospho-ERK, anti-ERK, anti-phospho-JNK, anti-JNK, anti-phospho-P38, and anti-P38 were obtained from Cell Signaling Technology (Beverly, MA); anti-FN was obtained from Sigma (St. Louis, MO); anti-collagen I and anti-α-SMA were obtained from Abcam (Cambridge, MA); and anti-GAPDH was obtained from Proteintech Group (Chicago, IL).

Table 1 The sequences of siRNAs

siRNAs	Sequences	5′-3′
siETS2-1#	Sense:	GCCUCAAUAAGCCAACCAUTT
	Antisense:	AUGGUUGGCUUAUUGAGGCTT
siETS2-2#	Sense:	GAGCUGCUAUCAGACAAAUTT
	Antisense:	AUUUGUCUGAUAGCAGCUCTT
siETS2-3#	Sense:	GCAAGGCAAACCAGUUAUATT
	Antisense:	UAUAACUGGUUUGCCUUGCTT
siJUNB	Sense:	ACAAGGUGAAGACGCUCAATT
	Antisense:	UUGAGCGUCUUCACCUUGUTT
siSmad3	Sense:	GGAGAAAUGGUGCGAGAAGTT
	Antisense:	CUUCUCGCACCAUUUCUCCTC
siERK	Sense:	GUGCUCUGCUUAUGAUAAUTT
	Antisense:	AUUAUCAUAAGCAGAGCACTT
siJNK	Sense:	AAAGAAUGUCCUACCUUCUTT
	Antisense:	AGAAGGUAGGACAUUCUUUTT
siP38	Sense:	GAAGCUCUCCAGACCAUUUTT
	Antisense:	AAAUGGUCUGGAGAGCUUCTT
siControl	Sense:	UUCUCCGAACGUGUCACGUTT
	Antisense:	ACGUGACACGUUCGGAGAATT

RNA extraction and quantitative real-time PCR

Total RNA was extracted from kidney tissues or HK2 cells using RNAiso Plus reagent (Takara, Japan) according to the manufacturer's instructions. Five hundred nanograms of total RNA was reversely transcribed using the PrimeScript™ RT reagent kit (Takara). In order to quantify mRNA levels of various genes, quantitative real-time PCR (qRT-PCR) was performed using SYBR Premix Ex Taq™ (Takara) on a LightCycler480 System (Roche, Basel, Switzerland). Relative mRNA levels were calculated after normalization with GAPDH. The sequences of specific primers are listed in Table 2.

Immunofluorescence staining for HK2 cells

HK2 cells were cultured in 12-well plates and fixed with 4% paraformaldehyde for 30 min, followed by permeabilization of 0.2% Triton X-100. The cells were incubated with specific primary antibodies against vimentin, α-SMA, and collagen I overnight at 4 °C. Subsequently, the primary antibodies were detected using Alexon 594 or Alexon 488-conjugated secondary antibodies (Invitrogen) and the nuclei were stained with 4′,6-diamidino-2-phenylindole. Cells were observed using an Olympus IX-71 fluorescence inverted microscope.

Luciferase reporter assay

Human genomic DNA was used as a template to amplify the human JUNB fragments covering about 2.1 kb of 5′ flanking sequence by PCR. We then inserted the PCR products into the pGL3.0 basic vector (Promega, Madison, WI) and confirmed efficient insertion by sequencing. To detect the potential binding sites, we cloned different

Table 2 Sequences of specific primers for qRT-PCR

Species	Gene	Forward primer (5′-3′)	Reverse primer (5′-3′)
Human	E-cadherin	CTGAGAACGAGGCTAACG	CCACCATCATCATTCAATATG
	N-cadherin	ACACTGGTGGCACTACTAAG	TACACAATACAGAGGCAAAG
	Vimentin	TGAACGCAAAGTGGAATC	AGGTCAGGCTTGGAAACA
	FN	CACCCTCACCAACCTCA	CCTCGGAACATCAGAAAC
	ETS2	CCAGCCTTTGACACCTTT	AAGCCTGTTGGCACTTCT
	JUNB	ACAAACTCCTGAAACCGAGCCT	CGAGCCCTGACCAGAAAAGTA
	GAPDH	ACTCAGCAACGACCCATACCTC	CGCTCCTATGTCCCAAGAAACT
Mouse	ETS2	GGATGGATGGGAGTTCAA	TTGCCCGAAGTCTTGTG
	E-cadherin	CAGTGAAGCGGCATCTAA	GCTGGGAAACATGAGCAG
	α-SMA	GTGCTATGTCGCTCTGGACTT TGA	ATGAAAGATGGCTGGAAGAGG GTC
	FN	TGCCTCGGGAATGGAAAG	ATGGTAGGTCTTCCCATCGTCATA
	JUNB	ACAAACTCCTGAAACCCACCT	TCTGATCCCTGACCCGAAA
	GAPDH	TCAACGACCCCTTCATTGAC	ATGCAGGGATGATGTTCTGG

Table 3 Sequences of specific primers for ChIP-qPCR

Species	Gene	Forward primer (5′-3′)	Reverse primer (5′-3′)
Human	JUNB-N	CCAGGCCGCTTACTAGCTTT	TCATGGGAGCTGAGTCCAGA
	JUNB-P1	TCCCGTAGGATCCGAGTGAC	AAACAGGCTGGGGAAAGAGC
	JUNB-P2	GCTCTTTCCCCAGCCTGTTT	ACCCTCCCCTATTGACCCTG
	JUNB-P3	CGTACCCCGAGGTCCTTTG	CGCTAGTCAGCCACGGAAG

constructs of 5′ deletion of human JUNB promoter or mutated seed sequences for ETS2-binding sites. For the luciferase reporter assay, HEK293T cells were cultured in 24-well plates and transfected each well with 0.5 µg firefly luciferase reporter plasmid, 0.05 µg pRL-CMV plasmid (Promega), and 0.5 µg control or Flag-ETS2 construct (Genechem Co., Ltd, Shanghai, China) using Lipofectamine 3000 (Invitrogen). Luciferase activities at 36 h after transfection were measured using luciferase assay kits (Promega).

Chromatin Immunoprecipitation (ChIP) analysis

ChIP assay was performed by Magna ChIP A/G Assay Kit (Millipore, Bedford, MA) according to the manufacturer's instruction. HK2 cells were treated with TGF-β1 for 24 h and fixed with 1% formaldehyde in DMEM for 10 min. Glycine was added to each dish and set for 5 min prior to washing in cold PBS two times. Cells were collected, resuspended, and sonicated to generate 200–800 bp DNA fragments. Immunoprecipitation was performed with IgG antibody (Cell Signaling, Beverly, MA) and ETS2 antibody (Santa Cruz, CA). Precipitated DNAs were measured by qRT-PCR using specific primers for either ETS binding sites or a non-ETS binding site on JUNB promoter. The sequences of specific primers are listed in Table 3.

Statistical analysis

All results were repeated at least three times. Experimental data were presented as mean ± SD. Differences between two groups were analyzed using a two-tailed unpaired Student's *t* test. Multiple comparisons were assessed using one-way analysis of variance. $P < 0.05$ was considered as statistically significant.

Results

ETS2 expression is elevated in the UUO-induced model of renal fibrosis

The unilateral ureteral obstruction (UUO) mouse model, a well-established model of experimental renal fibrosis, was set up to explore the role of ETS2 in renal fibrosis. Immunohistochemical staining revealed that ETS2 was drastically increased in the UUO-induced mouse kidney and was mainly located in the nuclear of dilated tubular cells (Fig. 1a). Meanwhile, we found a decrease of E-cadherin in renal tubules damaged and a significant increase of α-SMA and FN in renal tubulointerstitium at day 7 after UUO (Fig. 1a). Furthermore, qRT-PCR and western blot results showed that the levels of ETS2, α-SMA, and FN were significantly increased, while the level of E-cadherin was decreased in obstructed kidney compared with those in the sham group (Fig. 1b, c). These results suggest that ETS2 may be involved in the development of renal fibrosis.

TGF-β1 increases ETS2 expression in HK2 cells through Smad3 and ERK signaling pathways

Renal tubular epithelial cells that had undergone EMT were attributed to the development of renal fibrosis in a variety of CKDs [22, 23]. To determine the pathologic causes responsible for regulating ETS2 in diseased kidneys, HK2 cells were treated with TGF-β1. As shown in Fig. 2a, c, TGF-β1 treatment obviously reduced E-cadherin expression and increased the expression of N-cadherin and FN, indicating that the HK2 cells were undergoing EMT after exposure to TGF-β1. Meanwhile, ETS2 in HK2 cells was increased rapidly at both mRNA and protein levels in a dose- and time-dependent manner after TGF-β1 stimulation (Fig. 2a–d).

In order to explore the downstream signaling that mediates TGF-β1-induced ETS2 transcription, small molecules that specifically and respectively inhibit TGF-β type I receptor, Smad3, ERK1/2, JNK, and P38 were added to TGF-β1-treated HK2 cells. Silencing vectors targeting these signal molecules were also employed. Results revealed that TGF-β1-induced expression of ETS2 was largely reversed by TGF-β type I receptor inhibitor SB431542 or ERK inhibitor U0126, but not by Smad3 inhibitor SIS3, JNK inhibitor SP600125, or P38 inhibitor SB203580 (Fig. 3a, c, e, g). siRNA knockdown assays showed all siRNA constructs could effectively knockdown protein expressions, while silencing Smad3 or ERK1/2, but not JNK or P38, could obviously reduce the expression of ETS2 caused by TGF-β1 (Fig. 3b, d, f, h). These data indicate TGFβ1 increased ETS2 expression in HK2 cells via TGFβ/Smad and ERK signaling.

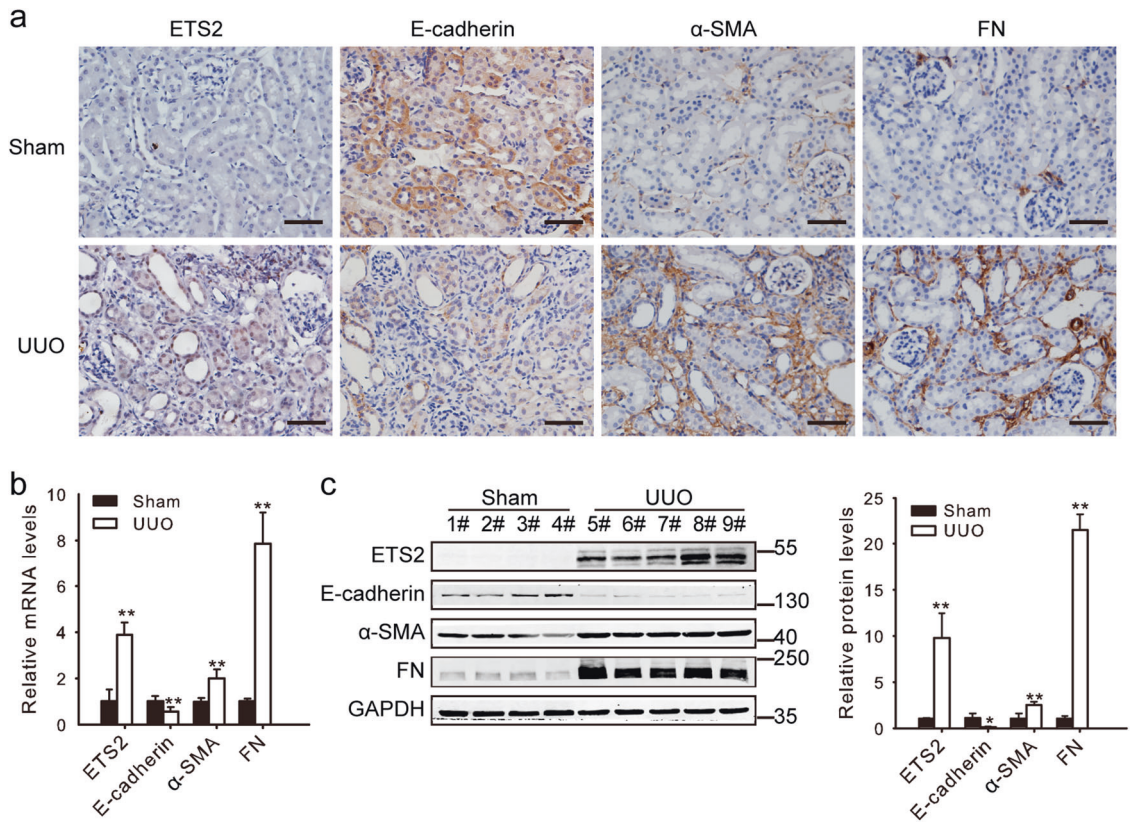

Fig. 1 ETS2 was elevated in mouse kidneys of the renal fibrosis model induced by unilateral ureteral obstruction (UUO). Representative images of immunohistochemical staining (**a**), quantitative real-time polymerase chain reaction (qRT-PCR) (**b**), western blot analyses and quantitative data (**c**) show the levels of ETS2, E-cadherin, α-SMA, and FN in sham and obstructed kidneys at day 7 after UUO. Scale bar = 50 μm. Numbers indicated each individual animal in a labeled group. Intensity of protein bands was normalized to GAPDH. Data are presented as mean ± SD from three independent experiments. $*P < 0.05$ and $**P < 0.01$ versus the sham group ($n = 6$)

ETS2 mediates TGF-β1-induced cell plasticity and the expressions of profibrotic factors in HK2 cells

We further evaluated whether the role of ETS2 in the occurrence of EMT in renal tubular epithelial cells after exposure to TGF-β1 and chronic injury. Three siRNA constructs against ETS2 and scramble control were synthesized and respectively transfected HK2 cells. Data demonstrated that the ETS2 mRNA level drastically decreased at 48 h after transfection with siRNA constructs targeting ETS2 in the absence or presence of TGF-β1 (Fig. 4a, b). According to the interference efficiency of different siRNA constructs, we chose siETS2-1# and siETS2-2# constructs to knockdown the ETS2 expression in the following experiments.

Notably, ETS2 silencing significantly repressed the TGF-β1-mediated induction of vimentin and FN at both the mRNA and protein levels (Fig. 4c, d). We also found ETS2 silencing reduced the protein expression of α-SMA, N-cadherin, and collagen I in HK2 cells exposed to TGF-β1 (Fig. 4d). Moreover, as shown in Fig. 4e, TGF-β1-treated cells exhibited a spindle shape compared with the cells without stimulation, but silencing ETS2 inhibited the change of cell shape induced by TGF-β1. Immunofluorescence staining also confirmed that silencing ETS2 expression significantly inhibited both the phenotypic conversion and the increased expression of vimentin, α-SMA, and collagen I in TGF-β1-treated HK2 cells (Fig. 4e). In contrast, overexpression of ETS2 with lentivirus plasmid promoted the TGF-β1-mediated induction of vimentin, N-cadherin, and FN in HK2 cells (Fig. 5). Taken together, these results indicate that ETS2 promotes TGF-β1-induced cell plasticity and the expression of profibrotic factors in HK2 cells.

ETS2 directly regulates the transcription of JUNB

In order to investigate the mechanism via which ETS2 promoted TGF-β1-induced EMT programming in HK2 cells, we took the advantage of JASPAR (http://jaspar.genereg.net/) bioinformatics algorithms to predict JUNB as one of the downstream target genes of ETS2. Western blot and quantitative data revealed that silencing ETS2 significantly decreased JUNB expression in HK2 cells,

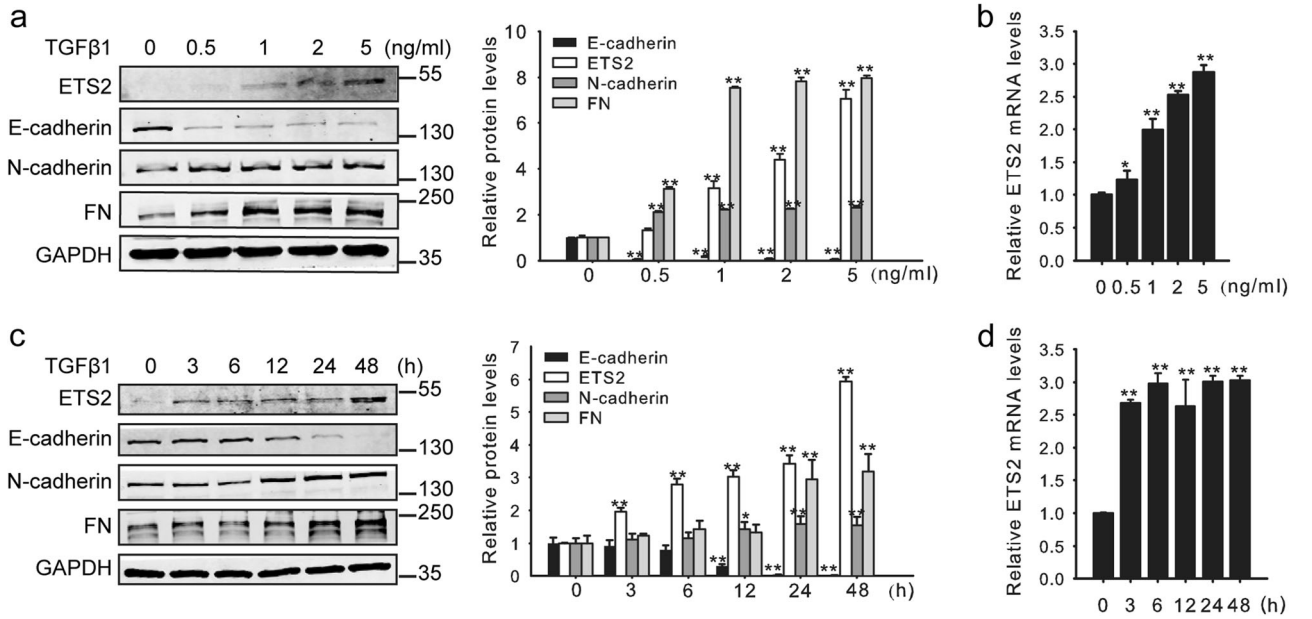

Fig. 2 TGFβ1 increased the expression of ETS2 and EMT markers in a dose- and time-dependent manner in HK2 cells. HK2 cells were incubated with the indicated dosage of TGFβ1 for 24 h (**a**, **b**) or 5 ng/ml TGFβ1 for various durations as indicated (**c**, **d**). Representative western blots and quantitative data show that TGFβ1 treatment reduced the expression of E-cadherin and increased the expression of ETS2, N-cadherin, and FN in HK2 cells (**a**, **c**). Relative protein levels (control = 1.0) are shown after normalization to GAPDH. Data are presented as mean ± SD from three independent experiments. $*P < 0.05$ and $**P < 0.01$ versus control

whereas overexpression of ETS2 resulted in an increase of JUNB in the absence or presence of TGF-β1 (Fig. 6).

We next performed luciferase reporter and ChIP-qPCR assays to validate that ETS2 could directly target the promoter region of JUNB. As shown in Fig. 7a, we inserted different fragments ranging from −1930 to +120 bp, the predicted promoter region of JUNB gene into the luciferase expressive PGL3.0 basic plasmid. Results showed that the luciferase activity significantly increased in HEK293T cells when co-transfected with ETS2 expression plasmid compared with control vector (Fig. 7a). Three truncated sequences that delete the predicted ETS2-binding motifs, namely ΔJUNB-1 (−1399 to +120 bp), ΔJUNB-2 (−949 to +120 bp), and ΔJUNB-3 (−349 to +120 bp), were separately subcloned and transfected HEK293T cells to search which portion of the JUNB promoter region is responsible for the transcriptional regulation by ETS2. The luciferase activities in the ΔJUNB-2 and ΔJUNB-3, but not ΔJUNB-1, constructs were reduced under treatment with ETS2 expressive vectors (Fig. 7a).

Among them, four ETS2-binding motifs were predicted in the −1399 to −949 bp region, and two existing in the −349 to +120 bp region, of the JUNB promoter. To determine which motif participates in the regulation of JUNB activity, we created an additional series of constructs containing mutant binding sites of JUNB, which were respectively designated as M1, M2, M3, M4, M5, and M6, as illustrated in Fig. 5f, g. In the presence of exogenous ETS2, the luciferase activity of ΔJUNB-1 construct significantly increased, whereas M3 and M4 rather than M1 or M2 resulted in the reduction in luciferase activity (Fig. 7b). Similarly, the luciferase activity of ΔJUNB-3 construct was enhanced by the overexpression of ETS2, whereas mutation of M5 but not M6 resulted in the significant reduction of luciferase activity (Fig. 7c). These findings clearly demonstrate that ETS2 induces the transcription of JUNB through three ETS2-binding site motifs.

ChIP-qPCR assays for ETS2 were performed with chromatin from HK2 cells treated with TGFβ1. Primers specific for domains of the terminal ETS binding site on JUNB promoter (JUNB-P1, JUNB-P2, and JUNB-P3) and a non-ETS2-binding site (JUNB-N) were designed. Results revealed that all three ETS binding sites could be enriched by ETS2 antibody (Fig. 7d). In addition, TGFβ1 strongly increased ETS2-binding to the ETS binding sites on JUNB promoter (Fig. 7d). These results confirmed the direct binding between ETS2 and JUNB promoter.

JUNB enhances TGF-β1-induced EMT in HK2 cells

Considering that JUNB is the direct target gene of ETS2 confirmed by TGF-β1 stimulation in HK2 cells, we next investigated the role of JUNB in TGF-β1 induced EMT. As expected, JUNB was prominently elevated in TGF-β1-treated HK2 cells, in a dose- and time-dependent manner (Fig. 8a–d), and also increased in UUO-induced mouse

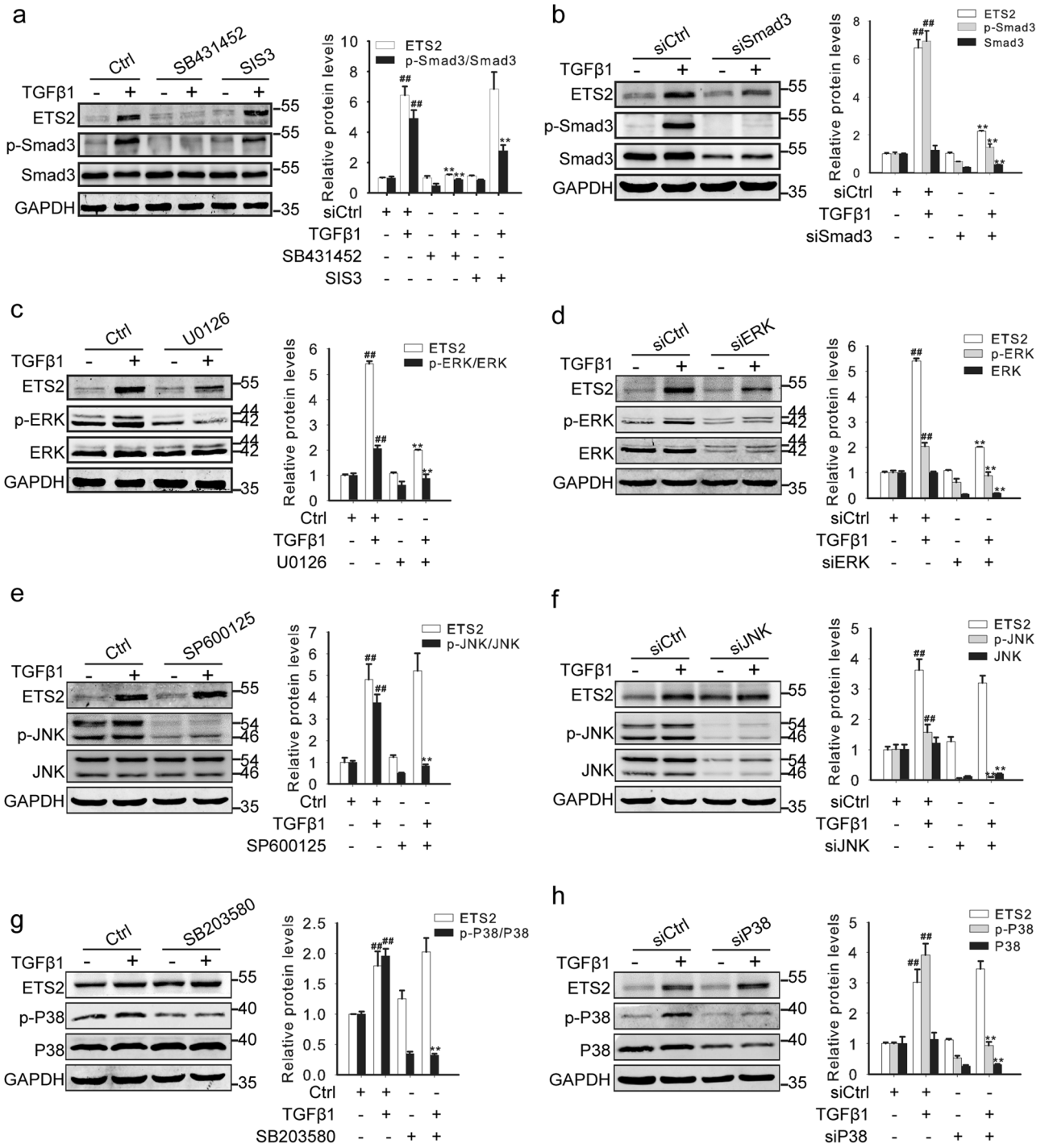

Fig. 3 TGFβ1 increased ETS2 expression in HK2 cells via TGFβ/Smad signaling and ERK signaling. HK2 cells were respectively pretreated with various inhibitors for 1 h, or transfected with various siRNAs for 24 h before incubation with TGFβ1. Representative western blots and quantitative data show that upregulation of ETS2 by TGFβ1 was inhibited by TGF-β type I receptor inhibitor (SB431542; 10 μM) (**a**), Smad3 siRNA (**b**), ERK inhibitor (U0126; 10 μM) (**c**), or ERK siRNA (**d**), but not by JNK inhibitor (SP600125; 10 μM) (**e**), JNK siRNA (**f**), P38 inhibitor (SB203580; 10 μM) (**g**), or P38 siRNA (**h**). Data are presented as mean ± SD from three independent experiments. $^{\#\#}P < 0.01$ versus control. $^{**}P < 0.01$ versus TGFβ1-treated cells

kidneys (Fig. 8e, f). siRNA fragment that successfully silenced endogenous JUNB (Fig. 9a) was employed in TGF-β1-treated HK2 cells. Data suggested that knockdown of JUNB obviously prevented the increment of vimentin, N-cadherin, collagen I, and FN due to TGF-β1 treatment (Fig. 9b). Furthermore, silencing JUNB expression drastically repressed TGF-β1-mediated EMT of HK2 cells and the expression of vimentin, α-SMA, and collagen I protein

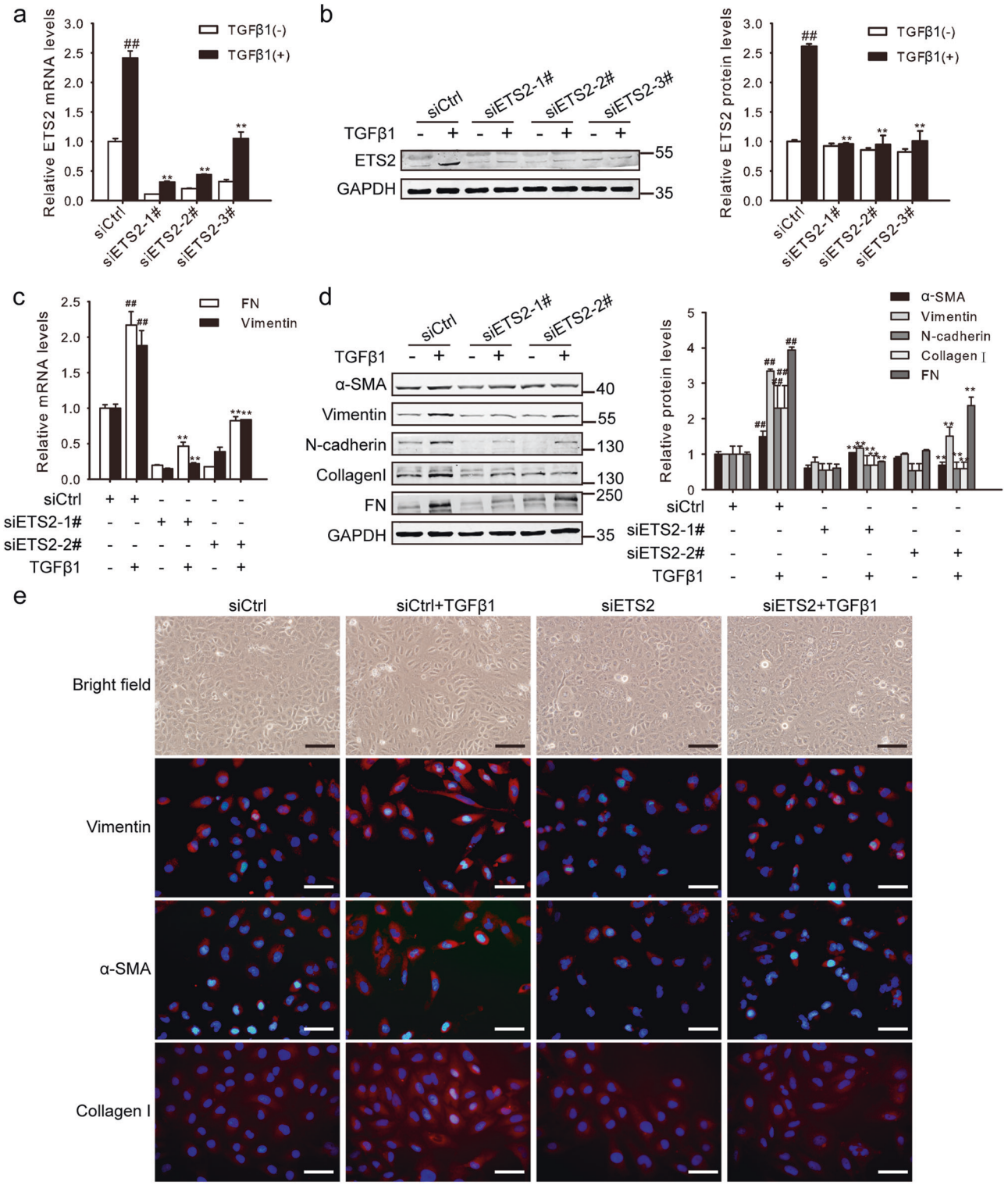

(Fig. 9c). In contrast, transfection of JUNB overexpression plasmid (Fig. 9d) promoted the TGF-β1-mediated induction of vimentin, N-cadherin, and FN in HK2 cells (Fig. 9e). These results demonstrate that JUNB mediates the TGF-β1-induced EMT in HK2 cells.

ETS2 regulates TGF-β1-induced EMT in HK2 cells via JUNB

In order to explore whether ETS2 targeting JUNB was responsible for its effects on TGF-β1-induced EMT in HK2

◀ **Fig. 4** Knockdown of ETS2 prevented TGFβ1-mediated induction of profibrotic factors in HK2 cells. HK2 cells were transfected with siRNA to silence ETS2 (siETS2) or scramble control (siCtrl) for 48 h, followed by treatment with TGFβ1 (5 ng/ml) for 24 h. The expression of ETS2 in HK2 cells was determined by qRT-PCR (**a**) and western blot (**b**). Quantitative data show that ETS2 expression was obviously inhibited in HK2 cells transfected with targeted siRNA. **c** qRT-PCR results show that knockdown of ETS2 expression reduced the elevated levels of vimentin and FN mRNA induced by TGFβ1. **d** Representative western blots and quantitative data show that TGFβ1 treatment increased the protein expression of α-SMA, vimentin, N-cadherin, collagen I, and FN, and knockdown of ETS2 prevented their expression. **e** Representative bright field images show that HK2 cells incubated with TGFβ1 exhibited an elongated morphology and ETS2 depletion inhibited the change of cell morphology. Representative immunofluorescence staining images reveal that ETS2 silencing significantly inhibited the enhanced expression of vimentin, α-SMA, and collagen I induced by TGFβ1 stimulation. Scale bar = 50 μm. Relative protein levels (control = 1.0) are shown after normalization to GAPDH. Data are presented as mean ± SD from three independent experiments. $^{\#\#}P < 0.01$ versus siCtrl. $^{**}P < 0.01$ versus siCtrl + TGFβ1

cells, the cells were co-transfected with lentivirus-encoding ETS2 and siJUNB, followed by TGF-β1 stimulation. Data revealed that knockdown of JUNB partially inhibited ETS2-mediated upregulation of the profibrogenic maker proteins N-cadherin and FN in HK2 cells, whereas claudin1 showed the opposite trend (Fig. 10). These results suggest that ETS2 regulates TGF-β1-induced EMT in HK2 cells through the transcription of JUNB.

Discussion

We believe for the first time that we uncover a significant upregulation of ETS2 expression in the kidney cortex of mice with UUO. We further provide evidence showing that ETS2 is induced in HK2 cells by TGF-β1 dependent on Smad3 and ERK signaling pathways and then contributes to TGF-β1-mediated EMT through the increased expression of fibrosis-related genes in HK2 cells. In addition, ETS2 binds to the promoter and starts the transcription of JUNB, which

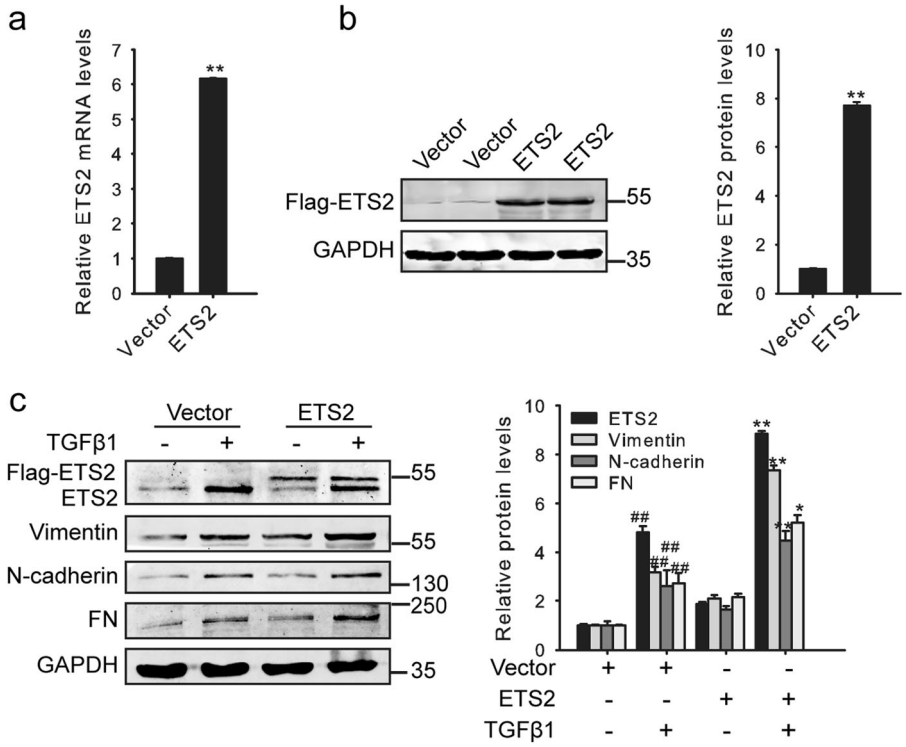

Fig. 5 Overexpression of ETS2 promoted the TGFβ1-mediated induction of profibrotic factors in HK2 cells. Cells were transfected with lentivirus-encoding ETS2 (ETS2) or flag (vector) for 96 h. ETS2 expression in HK2 cells was detected by qRT-PCR (**a**) and western blot (**b**). Quantitative data show that ETS2 expression was obviously increased in HK2 cells transfected with lentivirus-encoding ETS2. **c** Representative western blots and quantitative data show that ectopic expression of ETS2 promoted TGFβ1-mediated induction of vimentin, N-cadherin, and FN. HK2 cells were transfected with lentivirus-encoding ETS2, followed by TGFβ1 treatment (5 ng/ml) for 24 h. Relative protein levels (control = 1.0) are shown after normalization to GAPDH. Data are presented as mean ± SD from three independent experiments. $^{\#\#}P < 0.01$ versus vector. $^{*}P < 0.05$ and $^{**}P < 0.01$ versus vector + TGFβ1

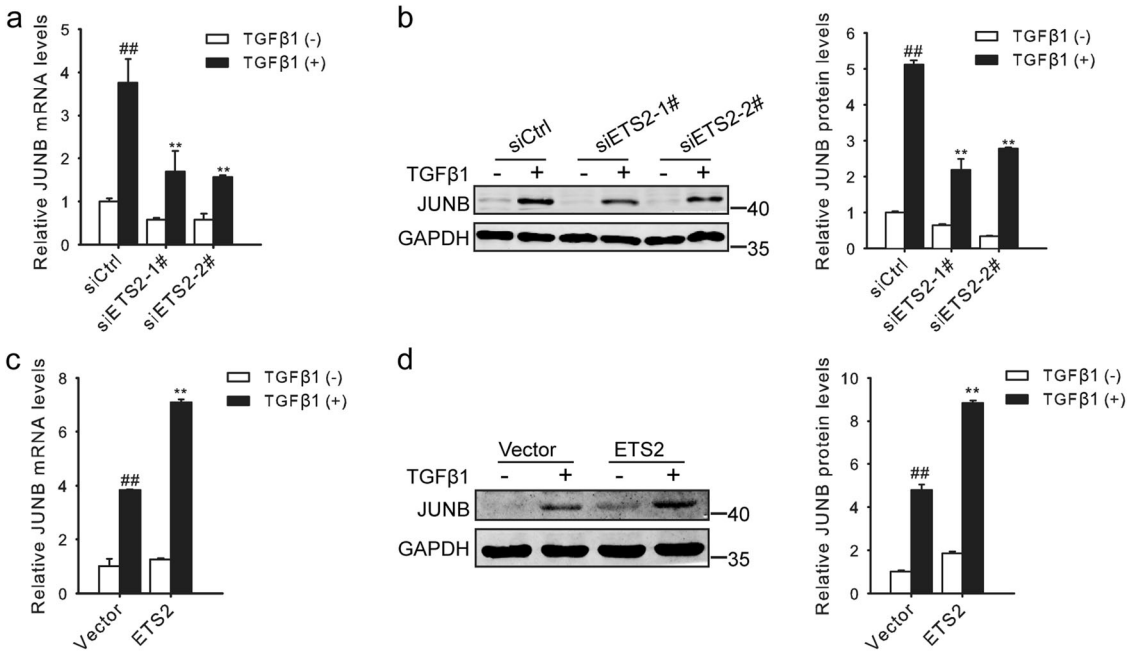

Fig. 6 ETS2 regulated the expression of JUNB in TGFβ1-treated HK2 cells. (**a**, **b**) Knockdown of ETS2 decreased JUNB mRNA and protein expression in HK2 cells with or without TGFβ1 treatment. Data are presented as mean ± SD from three independent experiments. $^{\#\#}P < 0.01$ versus siCtrl. $^{**}P < 0.01$ versus siCtrl + TGFβ1. (**c**, **d**) ETS2 overexpression increased JUNB mRNA and protein expression in HK2 cells with or without TGFβ1 treatment. Data are presented as mean ± SD from three independent experiments. $^{\#\#}P < 0.01$ versus vector. $^{**}P < 0.01$ versus vector + TGFβ1

is then responsible for TGF-β1-induced EMT (Fig. 11). Therefore, ETS2 plays a significantly important role in the EMT programming in HK2 cells and profibrotic responses. These findings suggest that ETS2 could be a novel target for discovering drugs to prevent the progression of renal fibrosis and benefit the patients with related disorders.

Renal fibrosis is the common feature of CKDs resulting from different etiologies. Much attention has been focused on resident intestinal fibroblasts that are the main producer of ECM components such as collagens and fibronectin to promote renal fibrosis [24, 25]. However, emerging evidence shows that tubular epithelial cells undergoing an EMT-like programming play a prominent role in the expansion of ECM deposits and fibrogenesis [7, 8]. In this study, we found a significant reduction of E-cadherin and robust increase of α-SMA and FN in UUO mice, which is consistent with previous studies [26]. There is no obvious expression of ETS2 in normal kidney, whereas ETS2 was observed to locate in the nuclear of renal tubular cells and obviously increase in the kidney cortex of mice after UUO. ETS2 is a transcription factor with broad expression in a variety of tissues. Overwhelming evidence confirms that ETS2 regulates ECM remodeling by mediating the expression of MMPs as well as uPA in response to various stimuli [27, 28]. A previous report demonstrates the phosphorylation of ETS2 at threonine-72 is of importance in human and murine pulmonary fibrotic response [19]. It is plausible to suggest that ETS2 may be at least partially involved in the development and progression of renal fibrosis.

Various cytokines and signaling pathways have been reported to regulate ETS2 in different tissues. In embryo and tumor development, ETS2 is activated by multiple signaling pathways, including Ras/MAPK [29–31], HGF-MET [32], and Wnt/β-catenin pathways [33]. However, we are still lacking knowledge about how ETS2 transcription mediates in the progression of renal fibrosis. In response to the activation of receptors by TGF-β1, Smad proteins are phosphorylated and then trigger transcription of target genes mediating fibrosis. It can also activate the MAPKs, including p38, JNK, and ERK, in a Smad-independent manner [34]. In this study, we uncovered that the expression of ETS2 induced by TGF-β1 was largely inhibited by TGF-β type I receptor or ERK inhibitor. Silencing assay also supports that ERK mediates TGF-β1-induced ETS2 expression. Meanwhile, the data from inhibitor and silencing assays targeting Smad3 are inconsist. We speculate that the maximum acceptable dosage of Smad3 inhibitor is not high enough to complete block its activity, which cause the ineffective reversal of TGF-β1-induced ETS2 expression. Instead, knockdown assay clearly shows the role of Smad3 in ETS2 induction. These data, when taken together, suggest that TGF-β1 induced ETS2 expression in renal tubular cells via a Smad3 and ERK pathways.

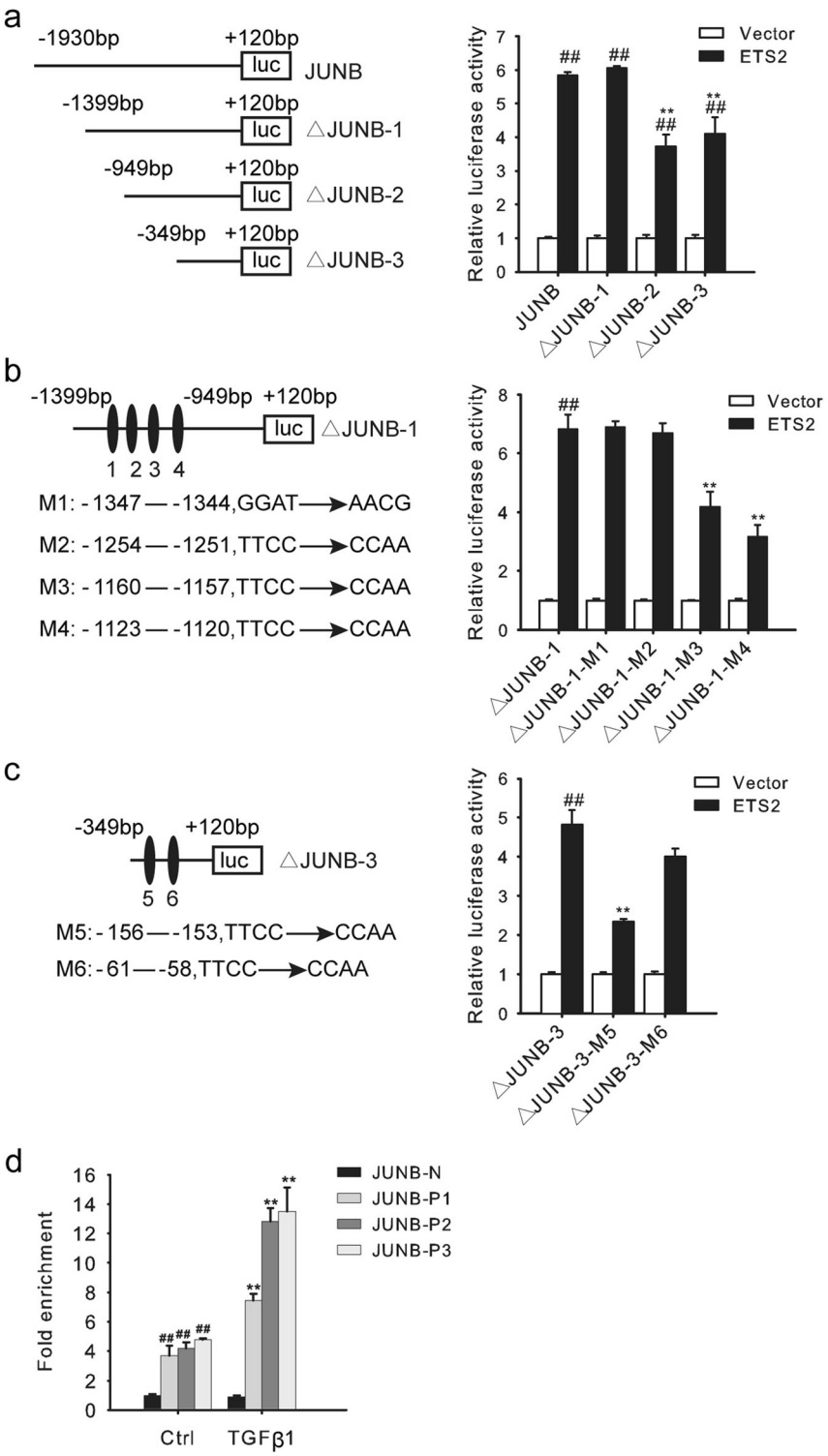

Fig. 7 JUNB is the direct target of ETS2. **a** Relative luciferase activity in HEK293T cells co-transfected with Flag-ETS2 or vector and the wild-type JUNB promoter (JUNB) or the different truncated JUNB constructs: △JUNB-1, △JUNB-2, and △JUNB-3. The left schematic diagram represents deletion constructs spanning from −1920 to +120 of human JUNB promoter. $^{\#\#}P < 0.01$ versus vector. $^{**}P < 0.01$ versus ETS2 + △JUNB. (**b**, **c**) HEK293T cells were transiently co-transfected with Flag-ETS2 or vector and wild-type or mutant constructs: M1 to M6, to test the promoter activity of △JUNB-1 and △JUNB-3. Schematic diagram shows the mutant sequences of six ETS2-binding sites of JUNB promoter. All data are presented as mean ± SD from three independent experiments. $^{\#\#}P < 0.01$ versus vector + △JUNB-1 and $^{**}P < 0.01$ versus ETS2 + △JUNB-1 in panel b. $^{\#\#}P < 0.01$ versus vector + △JUNB-3 and $^{**}P < 0.01$ versus ETS2 + △JUNB-3 in panel c. **d** ChIP assays for ETS2 were performed with chromatin from HK2 cells treated with TGFβ1 for 24 h. Primers specific for domains of the terminal ETS binding site on JUNB promoter (JUNB-P1, JUNB-P2 and JUNB-P3), and additionally a non-ETS2-binding site (JUNB-N) were designed. Binding events were measured as fold enrichment by quantitative real-time PCR. JUNB-P1:- 1222- -1128, JUNB-P2: -1148- -1039, JUNB-P3: -240- -44, JUNB-N: -739- -644. Data are presented as mean ± SD from three independent experiments. $^{\#\#}P < 0.01$ versus JUNB-N Control, and $^{**}P < 0.01$ versus JUNB-N TGFβ1

ETS2 is reported to be involved in the EMT programming in various carcinoma cells. In human non-small-cell lung cancer, ETS2 expression is negatively linked to the EMT-related genes such as ZEB1 and snail2 [15]. On the other hand, downregulation of ETS2 prevents the invasion and metastasis of renal cell carcinoma cells by mediating the increase of E-cadherin and the reduction of N-cadherin, ZEB1, ZEB2, and Snail [21]. Although TGF-β1 and ETS2 have been respectively reported to implicate in the process of EMT, we still lack mechanistic insight about the roles of ETS2 in TGF-β1-induced EMT. Our present work demonstrated that knockdown of ETS2 in HK2 cells greatly

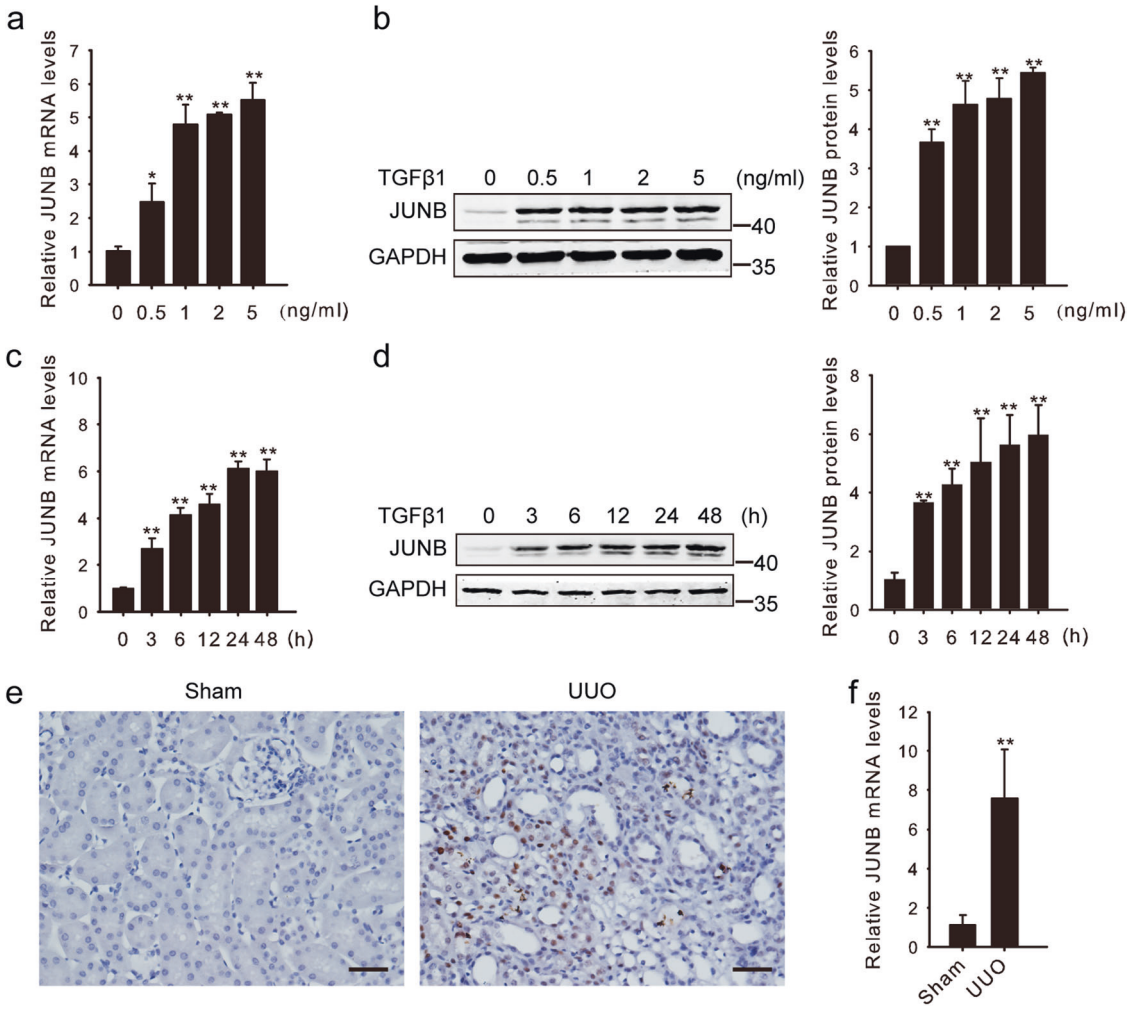

Fig. 8 The expression of JUNB was elevated in HK2 cells and UUO kidneys. HK2 cells were incubated with the indicated dosage of TGFβ1 for 24 h (**a**, **b**) or 5 ng/ml TGFβ1 for various durations as indicated (**c**, **d**). Relative protein levels (control = 1.0) are shown after normalization to GAPDH. $*P < 0.05$; $**P < 0.01$ versus control. **e** Representative images of immunohistochemical staining of JUNB in sham and obstructed kidneys at day 7 after UUO. Scale bar = 50 μm. **f** qRT-PCR results show levels of JUNB in sham and obstructed kidneys at day 7 after UUO. Data are presented as mean ± SD from three independent experiments. $**P < 0.01$ versus sham group ($n = 6$)

attenuated TGF-β1-induced morphologic change from the typical epithelial type to a fibroblastic appearance. Importantly, the expressions of mesenchymal markers (vimentin, N-cadherin, and α-SMA) and ECM proteins (collagen I and FN) were reduced by downregulation of ETS2 in the presence of TGF-β1. These results support that ETS2 plays a crucial role in the onset of TGF-β1-induced EMT programming in renal tubular cells.

Cumulative studies reveal that ETS2 is not working alone but interacts with a lot of requisite partners such as nuclear factor-κB and AP-1 to regulate gene expression and affect biological functions [35, 36]. In a previous study, ETS2 in cooperation with c-Jun enhances Syk expression and promotes Syk-mediated calcium response in SLE T cells [37]. However, it is reported that the dichotomy of ETS2 transcriptional activity exists in various cell lines. The discovery of ETS2 downstream target genes is of significant importance to expand our knowledge regarding the mechanism based on the contribution of ETS2 to regulating the EMT programming. Interestingly, Chang et al. [38] indicate that ETS2, HNF4A, and JUNB are associated with super-enhancers and cooperatively regulate numerous key EMT genes in small lung cancer A549 cells with TGF-β1 treatment. In this study, we also found that knockdown or overexpression of ETS2 obviously reduced or increased the expression of JUNB. Based on the luciferase reporter and ChIP assays, we further identify that ETS2 binds to the promoter of JUNB, through which, promotes the expression of JUNB. How ETS2 and other cooperative partners cooperatively bind to promoter and regulate JUNB is not observed and deserves further investigation.

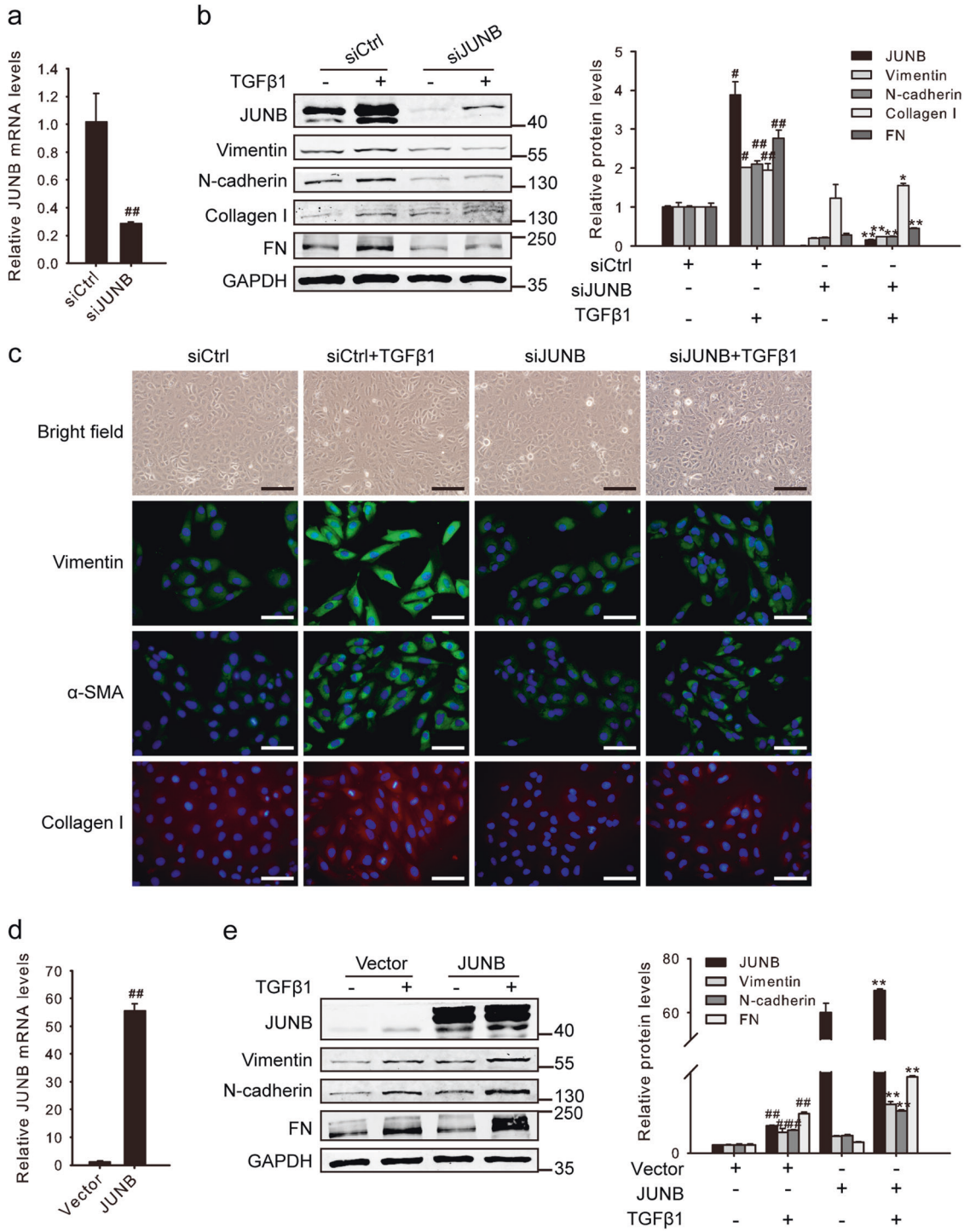

Fig. 9 JUNB was essential for TGFβ1-mediated induction of various profibrotic factors in HK2 cells. **a** qRT-PCR analyses of the expression of JUNB in HK2 cells at 48 h after transfection with siRNA fragment. **b** Knockdown of JUNB expression prevented the increased expression of vimentin, N-cadherin, collagen I, and FN in HK2 cells with TGFβ1 treatment. $^{\#}P < 0.05$ and $^{\#\#}P < 0.01$ versus siCtrl. $^{*}P < 0.05$ and $^{**}P < 0.01$ versus siCtrl + TGFβ1. **c** Representative bright field images and immunofluorescence staining images show HK2 cells incubated with TGFβ1 exhibited an elongated shape, while JUNB depletion inhibited the change of cell morphology and the enhanced expression of vimentin, α-SMA, and collagen I induced by TGFβ1 stimulation. Scale bar = 50 μm. **d** qRT-PCR analyses of the expression of JUNB in HK2 cells at 48 h after transfection with JUNB plasmid. **e** Representative western blots and quantitative data show that ectopic expression of JUNB promoted the increased expression of vimentin, N-cadherin, and FN in HK2 cells with TGFβ1 treatment. Relative protein levels (control = 1.0) are shown after normalization to GAPDH. Data are presented as mean ± SD from three independent experiments. $^{\#\#}P < 0.01$ versus vector. $^{**}P < 0.01$ versus vector + TGFβ1

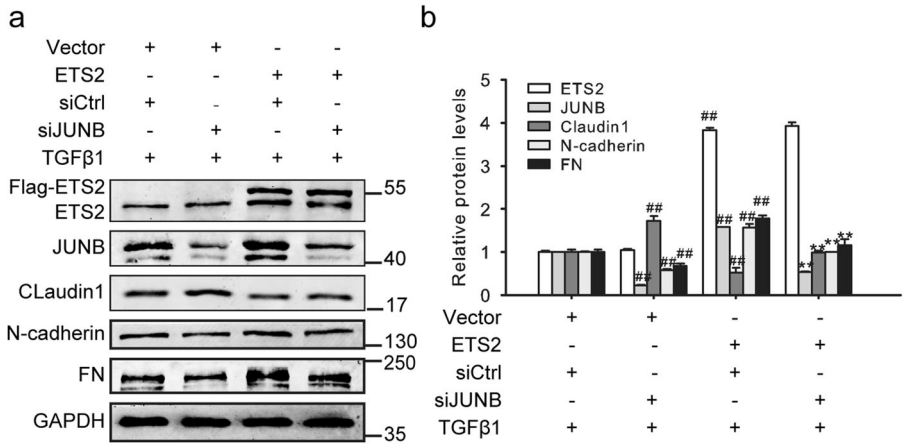

Fig. 10 ETS2 regulated TGFβ1-mediated expression of EMT marker proteins through JUNB in HK2 cells. HK2 cells were transfected with lentivirus-encoding ETS2 and siJUNB fragment, followed by treatment with TGFβ1 for 24 h. JUNB silencing attenuated the effect of ETS2 on TGFβ1-mediated expression of claudin1, N-cadherin, and FN by western blot (**a**) and quantitative analyses (**b**). Relative protein levels (control = 1.0) are shown after normalization to GAPDH. Data are presented as mean ± SD from three independent experiments. $^{\#\#}P < 0.01$ versus vector + siCtrl + TGFβ1. $^{**}P < 0.01$ versus ETS2 + siCtrl + TGFβ1

Expression of JUNB has been reported to increase in various cell lines exposed to TGF-β1 [39–41]. Consistent with previous studies, we found the expression of JUNB induced by TGF-β1 markedly increased in HK2 cells. JUNB has been implicated in cell adhesion, actin fibers, and matrix deposition in a variety of cell types [42–44]. JUNB can modulate myosin and the actin cytoskeleton to regulate TGF-β1-induced smooth muscle cell contractility [40]. In addition, a recent study by Gervasi et al. [39] demonstrates that JUNB is critical for upregulation of the key components of cell-matrix adhesion and actin stress fibers, including Itgb3, tropomyosin, and ezrin, which are involved in EMT and fibrosis. Moreover, JUNB enhances the production and transcription of FN in NMuMG cells with TGF-β1 treatment. In our present study, JUNB positively regulated the expression of mesenchymal markers as well as ECM proteins. These data suggest that JUNB and ETS2 may play a similar role in the TGF-β1-induced EMT programming in HK2 cells. We further confirmed that JUNB reduced the enhanced effects of ETS2 on TGF-β1-induced EMT programming in HK2 cells, showing that ETS2 may promote JUNB to regulate TGF-β1-induced EMT programming in HK2 cells.

In conclusion, ETS2 significantly increases in the renal fibrosis models and contributes to the TGF-β1-induced EMT programming in HK2 cells via transcription of JUNB. Inhibition of ETS2 in renal tubular epithelial cells may attenuate the development of renal fibrosis and protect the kidney from fibrotic injuries. An additional experiment is necessary to further validate the role and mechanism of ETS2 in the development of renal fibrosis using a genetic knockout mouse model and samples of clinical CKD patients, providing credible evidence for discovering drugs to stall, terminate, and reverse the progression of renal fibrosis and benefit CKD patients.

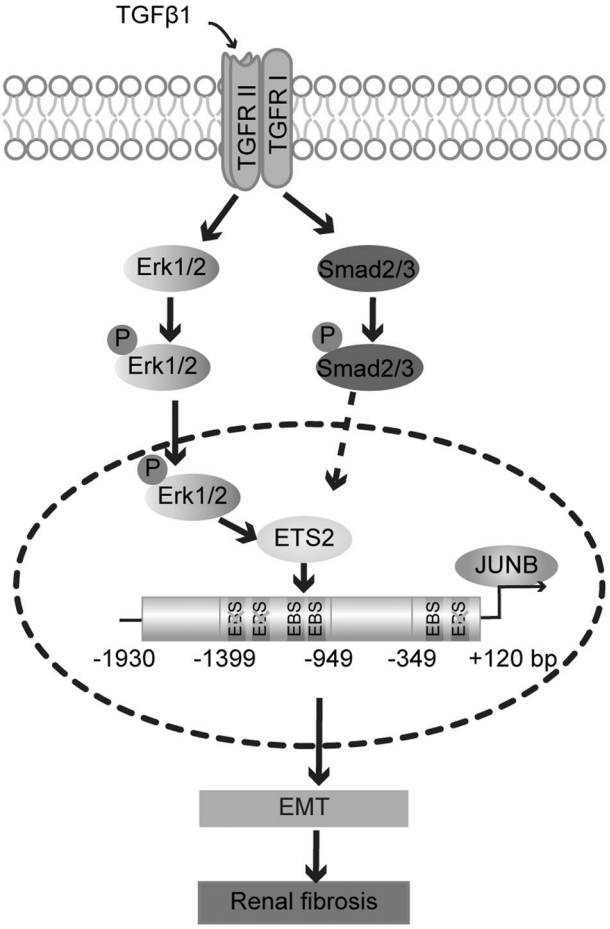

Fig. 11 Schematic model indicating ETS2 promotes EMT via targeting JUNB transcription in response to TGF-β1. TGF-β1 induces the expression of ETS2 in renal tubular cells through smad3 and ERK signaling. Notably, ETS2 mediates the transcription of JUNB by binding to three EBS motifs on its promoter, which contributes to the regulation of proteins that are essential for TGF-β1-induced EMT. The process may play an important role in the formation of renal fibrosis

Acknowledgements ETS2 antibody was obtained from Professor Peng Wang, Laboratory of Systems Biology, Shanghai Advanced Research Institute, Chinese Academy of Sciences.

Funding This work was supported by grants from National Natural Science Foundation of China (31529002), the State Key Development Program for Basic Research of China (2015CB553602), and scientific initiation program of Southern Medical University (C1051313).

Author contributions FY, Z-K C, BW, and XB, designed the experiment, analyzed data and wrote the manuscript; FY, XW, XA, JY, performed the experiments; FY, Z-K C, HL, QS and ZC, analyzed data and prepared figures. All authors approved the final version of the manuscript.

Compliance with ethical standards

Conflict of interest The authors declare that they have no conflict of interest.

Publisher's note Springer Nature remains neutral with regard to jurisdictional claims in published maps and institutional affiliations.

References

1. Eddy AA. Overview of the cellular and molecular basis of kidney fibrosis. Kidney Int Suppl. 2011;2014:2–8.
2. Liu Y. Cellular and molecular mechanisms of renal fibrosis. Nat Rev Nephrol. 2011;7:684–96.
3. Bohle A, Muller GA, Wehrmann M, Mackensen-Haen S, Xiao JC. Pathogenesis of chronic renal failure in the primary glomerulopathies, renal vasculopathies, and chronic interstitial nephritides. Kidney Int Suppl. 1996;54:S2–9.
4. Grande MT, Lopez-Novoa JM. Fibroblast activation and myofibroblast generation in obstructive nephropathy. Nat Rev Nephrol. 2009;5:319–28.
5. Boor P, Ostendorf T, Floege J. Renal fibrosis: novel insights into mechanisms and therapeutic targets. Nat Rev Nephrol. 2010;6:643–56.
6. Zeisberg M, Neilson EG. Mechanisms of tubulointerstitial fibrosis. J Am Soc Nephrol. 2010;21:1819–34.
7. Grande MT, Sanchez-Laorden B, Lopez-Blau C, De Frutos CA, Boutet A, Arevalo M, et al. Snail1-induced partial epithelial-to-mesenchymal transition drives renal fibrosis in mice and can be targeted to reverse established disease. Nat Med. 2015;21:989–97.
8. Lovisa S, LeBleu VS, Tampe B, Sugimoto H, Vadnagara K, Carstens JL, et al. Epithelial-to-mesenchymal transition induces cell cycle arrest and parenchymal damage in renal fibrosis. Nat Med. 2015;21:998–1009.
9. Meng XM, Nikolic-Paterson DJ, Lan HY. TGF-β: the master regulator of fibrosis. Nat Rev Nephrol. 2016;12:325–38.
10. Ding Y, Kim SL, Lee SY, Koo JK, Wang Z, Choi ME. Autophagy regulates TGF-beta expression and suppresses kidney fibrosis induced by unilateral ureteral obstruction. J Am Soc Nephrol. 2014;25:2835–46.
11. Zheng Z, Guan M, Jia Y, Wang D, Pang R, Lv F, et al. The coordinated roles of miR-26a and miR-30c in regulating TGFbeta1-induced epithelial-to-mesenchymal transition in diabetic nephropathy. Sci Rep. 2016;6:37492.
12. Seth A, Watson DK. ETS transcription factors and their emerging roles in human cancer. Eur J Cancer. 2005;41:2462–78.
13. Sharrocks AD. The ETS-domain transcription factor family. Nat Rev Mol Cell Biol. 2001;2:827–37.
14. Islas JF, Liu Y, Weng KC, Robertson MJ, Zhang S, Prejusa A, et al. Transcription factors ETS2 and MESP1 transdifferentiate human dermal fibroblasts into cardiac progenitors. Proc Natl Acad Sci USA. 2012;109:13016–21.
15. Kabbout M, Garcia MM, Fujimoto J, Liu DD, Woods D, Chow CW, et al. ETS2 mediated tumor suppressive function and MET oncogene inhibition in human non-small cell lung cancer. Clin Cancer Res. 2013;19:3383–95.
16. Sheydina A, Volkova M, Jiang L, Juhasz O, Zhang J, Tae HJ, et al. Linkage of cardiac gene expression profiles and ETS2 with lifespan variability in rats. Aging Cell. 2012;11:350–9.
17. Liao YL, Hu LY, Tsai KW, Wu CW, Chan WC, Li SC, et al. Transcriptional regulation of miR-196b by ETS2 in gastric cancer cells. Carcinogenesis. 2012;33:760–9.
18. Trojanowska M. Ets factors and regulation of the extracellular matrix. Oncogene. 2000;19:6464–71.
19. Baran CP, Fischer SN, Nuovo GJ, Kabbout MN, Hitchcock CL, Bringardner BD, et al. Transcription factor ets-2 plays an important role in the pathogenesis of pulmonary fibrosis. Am J Respir Cell Mol Biol. 2011;45:999–1006.
20. Wei G, Guo J, Doseff AI, Kusewitt DF, Man AK, Oshima RG, et al. Activated Ets2 is required for persistent inflammatory responses in the motheaten viable model. J Immunol. 2004;173:1374–9.
21. Zhang GW, Tian X, Li Y, Wang ZQ, Li XD, Zhu CY. Downregulation of ETS2 inhibits the invasion and metastasis of renal cell carcinoma cells by inducing EMT via the PI3K/Akt signaling pathway. Biomed Pharmacother. 2018;104:119–26.
22. Holian J, Qi W, Kelly DJ, Zhang Y, Mreich E, Pollock CA, et al. Role of Kruppel-like factor 6 in transforming growth factor-beta1-induced epithelial-mesenchymal transition of proximal tubule cells. Am J Physiol Renal Physiol. 2008;295:F1388–96.
23. Bedi S, Vidyasagar A, Djamali A. Epithelial-to-mesenchymal transition and chronic allograft tubulointerstitial fibrosis. Transplant Rev (Orlando). 2008;22:1–5.
24. Nishitani Y, Iwano M, Yamaguchi Y, Harada K, Nakatani K, Akai Y, et al. Fibroblast-specific protein 1 is a specific prognostic marker for renal survival in patients with IgAN. Kidney Int. 2005;68:1078–85.
25. Mack M, Yanagita M. Origin of myofibroblasts and cellular events triggering fibrosis. Kidney Int. 2015;87:297–307.
26. Zhou L, Li Y, Zhou D, Tan RJ, Liu Y. Loss of Klotho contributes to kidney injury by derepression of Wnt/beta-catenin signaling. J Am Soc Nephrol. 2013;24:771–85.
27. Cirillo G, Casalino L, Vallone D, Caracciolo A, De Cesare D, Verde P. Role of distinct mitogen-activated protein kinase pathways and cooperation between Ets-2, ATF-2, and Jun family members in human urokinase-type plasminogen activator gene induction by interleukin-1 and tetradecanoyl phorbol acetate. Mol Cell Biol. 1999;19:6240–52.
28. Watabe T, Yoshida K, Shindoh M, Kaya M, Fujikawa K, Sato H, et al. The Ets-1 and Ets-2 transcription factors activate the promoters for invasion-associated urokinase and collagenase genes in response to epidermal growth factor. Int J Cancer. 1998;77:128–37.
29. Galang CK, García-Ramírez J, Solski PA, Westwick JK, Der CJ, Neznanov NN, et al. Oncogenic Neu/ErbB-2 increases ets, AP-1, and NF-kappaB-dependent gene expression, and inhibiting ets activation blocks Neu-mediated cellular transformation. J Biol Chem. 1996;271:7992–8.
30. Yang BS, Hauser CA, Henkel G, Colman MS, Van Beveren C, Stacey KJ, et al. Ras-mediated phosphorylation of a conserved threonine residue enhances the transactivation activities of c-Ets1 and c-Ets2. Mol Cell Biol. 1996;16:538–47.
31. Foulds CE, Nelson ML, Blaszczak AG, Graves BJ. Ras/mitogen-activated protein kinase signaling activates Ets-1 and Ets-2 by CBP/p300 recruitment. Mol Cell Biol. 2004;24:10954–64.

32. Takeda S, Liu H, Sasagawa S, Dong Y, Trainor PA, Cheng EH, et al. HGF-MET signals via the MLL-ETS2 complex in hepatocellular carcinoma. J Clin Invest. 2013;123:3154–65.
33. Ye X, Hemida MG, Qiu Y, Hanson PJ, Zhang HM, Yang D. MiR-126 promotes coxsackievirus replication by mediating cross-talk of ERK1/2 and Wnt/β-catenin signal pathways. Cell Mol Life Sci. 2013;70:4631–44.
34. Meng XM, Nikolic-Paterson DJ, Lan HY. TGF-beta: the master regulator of fibrosis. Nat Rev Nephrol. 2016;12:325–38.
35. Smith JL, Schaffner AE, Hofmeister JK, Hartman M, Wei G, Forsthoefel D, et al. Ets-2 is a target for an akt (Protein kinase B)/jun N-terminal kinase signaling pathway in macrophages of motheaten-viable mutant mice. Mol Cell Biol. 2000;20:8026–34.
36. Majumder S, Roy S, Kaffenberger T, Wang B, Costinean S, Frankel W, et al. Loss of metallothionein predisposes mice to diethylnitrosamine-induced hepatocarcinogenesis by activating NF-kappaB target genes. Cancer Res. 2010;70:10265–76.
37. Ghosh D, Tsokos GC, Kyttaris VC. c-Jun and Ets2 proteins regulate expression of spleen tyrosine kinase in T cells. J Biol Chem. 2012;287:11833–41.
38. Chang H, Liu Y, Xue M, Liu H, Du S, Zhang L, et al. Synergistic action of master transcription factors controls epithelial-to-mesenchymal transition. Nucleic Acids Res. 2016;44:2514–27.
39. Gervasi M, Bianchi-Smiraglia A, Cummings M, Zheng Q, Wang D, Liu S, et al. JunB contributes to Id2 repression and the epithelial-mesenchymal transition in response to transforming growth factor-β. J Cell Biol. 2012;196:589–603.
40. Ramachandran A, Gangopadhyay SS, Krishnan R, Ranpura SA, Rajendran K, Ram-Mohan S, et al. JunB mediates basal- and TGFβ1-induced smooth muscle cell contractility. PLoS One. 2013;8:e53430.
41. Gokulnath M, Swetha R, Thejaswini G, Shilpa P, Selvamurugan N. Transforming growth factor-β1 regulation of ATF-3, c-Jun and JunB proteins for activation of matrix metalloproteinase-13 gene in human breast cancer cells. Int J Biol Macromol. 2016;94:370–7.
42. Ponticos M, Papaioannou I, Xu S, Holmes AM, Khan K, Denton CP, et al. Failed degradation of JunB contributes to overproduction of type I collagen and development of dermal fibrosis in patients with systemic sclerosis. Arthritis Rheumatol. 2015;67:243–53.
43. Busnadiego O, González-Santamaría J, Lagares D, Guinea-Viniegra J, Pichol-Thievend C, Muller L, et al. LOXL4 is induced by transforming growth factor β1 through Smad and JunB/Fra2 and contributes to vascular matrix remodeling. Mol Cell Biol. 2013;33:2388–401.
44. Sullivan BP, Kassel KM, Manley S, Baker AK, Luyendyk JP. Regulation of transforming growth factor-β1-dependent integrin β6 expression by p38 mitogen-activated protein kinase in bile duct epithelial cells. J Pharmacol Exp Ther. 2011;337:471–8.